Configuration and bandhead spin assignments for the two-quasiparticle rotational bands in the neutron-rich nuclei ^{154,156}Pm

Shuo-Yi Liu (刘硕一),[1] Miao Huang (黄苗),[1] and Zhen-Hua Zhang (张振华)[1,2,*]

[1]*Mathematics and Physics Department, North China Electric Power University, Beijing 102206, China*

[2]*Department of Physics and Astronomy, Mississippi State University, Mississippi 39762, USA*

(Received 17 June 2019; published 9 December 2019)

The rotational bands in the neutron-rich nuclei $^{153-157}$Pm are investigated by a particle-number-conserving method. The kinematic moments of inertia for the one-quasiparticle bands in odd-A Pm isotopes ^{153,155,157}Pm are reproduced quite well by the present calculation. By comparison between the experimental and calculated moments of inertia for the three two-quasiparticle bands in the odd-odd nuclei ^{154,156}Pm, their configurations and bandhead spins have been assigned properly. For the two-quasiparticle band in ^{154}Pm, the configuration is assigned as $\pi 5/2^-[532] \otimes \nu 3/2^-[521]$ ($K^\pi = 4^+$) with the bandhead spin $I_0 = 4\hbar$. In ^{156}Pm, the same configuration and bandhead spin assignments have been made for the two-quasiparticle band with lower excitation energy. The configuration $\pi 5/2^+[413] \otimes \nu 5/2^+[642]$ ($K^\pi = 5^+$) with the bandhead spin $I_0 = 5\hbar$ is assigned for that with higher excitation energy.

DOI: 10.1103/PhysRevC.100.064307

I. INTRODUCTION

Spectroscopic investigation of the neutron-rich nuclei around $A \approx 150$–160 mass region is quite challenging because it is very hard to find an appropriate combination of projectile and target to produce these nuclei in the fusion-evaporation reaction with sufficiently large cross section. Fortunately, the isomeric and high-spin states of these neutron-rich nuclei can be produced with high efficiency in the spontaneous fission of the actinide nuclei [1,2], by which various high-K isomers and high-spin rotational bands for the neutron-rich nuclei in this mass region have been established up to now. These data can provide detailed information on the nuclear phenomena such as K-isomerism, quantum phase transition, and octupole correlations, thus providing a benchmark for various available nuclear models [3–8].

As for the Pm ($Z = 61$) isotopes, a lot of effort has been put into the search for the parity doublet bands in order to investigate the reflection-asymmetric shape in this transitional mass region. Up to now, parity doublet bands in Pm isotopes have been observed in ^{147}Pm [9], ^{149}Pm [10], and ^{151}Pm [11,12]. Recently, high-spin structures in the neutron-rich $^{152-158}$Pm isotopes, including both odd-A and odd-odd nuclei, have been observed experimentally by the spontaneous fission of the actinide nuclei [13]. Compared with previous experiments [14–20], these rotational bands either have been obtained for the first time or have been extended considerably to higher spins. Unfortunately, these experimental data do not show any evidence of existing of octupole deformation in these Pm isotopes with neutron number $N > 90$. In Ref. [13], the configurations for the one-quasiparticle (1-qp) rotational bands in odd-A Pm isotopes have been assigned properly by the cranked relativistic Hartree-Bogoliubov calculations. Compared to odd-A nuclei, the structure of odd-odd nuclei is more complicated because of the contributions from both valence neutrons and protons. Note that in Refs. [21–23], some configurations for the 2-qp isomeric states in ^{154,156}Pm have already been suggested by the quasiparticle-rotor model. However, because of the lack of firm spin and parity assignments, reasonable configurations have not been assigned for these 2-qp rotational bands in odd-odd Pm isotopes in Ref. [13]. In the present work, the cranked shell model (CSM) with pairing correlations treated by a particle-number-conserving (PNC) method [24,25] will be used for investigating the rotational bands in these Pm isotopes, and the configuration and bandhead spin assignments will be made for the three 2-qp bands observed in ^{154,156}Pm. Note that PNC-CSM has already been used for the systematic investigation of the high-K isomers and high-spin rotational bands in the neighboring neutron-rich Nd ($Z = 60$), Sm ($Z = 62$), and Gd ($Z = 64$) isotopes [26,27], in which the experimental data are reproduced quite well. Therefore, the calculations for Pm isotopes by PNC-CSM should be quite reliable.

Unlike the conventional Bardeen-Cooper-Schrieffer or Hartree-Fock-Bogoliubov method, in the PNC method, the pairing Hamiltonian is diagonalized directly in a properly truncated Fock space [28]. Therefore, the particle number is totally conserved and the Pauli blocking effects are treated exactly, and it is very suitable for the investigation of the multi-qp rotational bands. Note that the PNC method has also been transplanted in the total-Routhian-surface method [29], and both relativistic [30,31] and nonrelativistic mean-field models [32]. Similar exact particle-number-conserving approaches can be found in Refs. [33–38].

*zhzhang@ncepu.edu.cn

This paper is organized as follows. The theoretical framework of PNC-CSM is presented briefly in Sec. II. In Sec. III, the moments of inertia (MOIs) of the rotational bands in Pm isotopes are calculated and compared with the data. The configuration and bandhead spin assignments for the three 2-qp bands in odd-odd nuclei ^{154,156}Pm are made. A brief summary is given in Sec. IV.

II. THEORETICAL FRAMEWORK

The cranked shell model Hamiltonian with pairing correlations can be written as

$$H_{\rm CSM} = H_0 + H_{\rm P} = H_{\rm Nil} - \omega J_x + H_{\rm P} \,, \tag{1}$$

where $H_{\rm Nil}$ is the Nilsson Hamiltonian [39] and $-\omega J_x$ is the Coriolis interaction with the cranking frequency ω about the x axis. $H_{\rm P} = H_{\rm P}(0) + H_{\rm P}(2)$ is the pairing Hamiltonian with monopole and quadrupole pairing interaction,

$$H_{\rm P}(0) = -G_0 \sum_{\xi\eta} a^\dagger_\xi a^\dagger_{\bar\xi} a_{\bar\eta} a_\eta \,, \tag{2}$$

$$H_{\rm P}(2) = -G_2 \sum_{\xi\eta} q_2(\xi) q_2(\eta) a^\dagger_\xi a^\dagger_{\bar\xi} a_{\bar\eta} a_\eta \,, \tag{3}$$

where $\bar\xi$ ($\bar\eta$) is the time-reversal state of ξ (η), $q_2(\xi) = \sqrt{16\pi/5}\langle\xi|r^2 Y_{20}|\xi\rangle$ is the diagonal element of the stretched quadrupole operator, and G_0 and G_2 are the effective monopole and quadrupole pairing strengths.

In the PNC method, the pairing Hamiltonian $H_{\rm P}$ is diagonalized directly in a sufficiently large cranked many-particle configuration (CMPC, an eigenstate of the one-body Hamiltonian H_0) space [24]. Instead of the traditional single-particle level truncation used in shell-model calculation, a CMPC truncation is adopted, which can make the PNC calculation both workable and accurate [28,40]. For the investigation of rare-earth nuclei, usually a CMPC space with the dimension of 1000 is enough. The eigenstates of $H_{\rm CSM}$ can be obtained by diagonalization in the truncated CMPC space

$$|\Psi\rangle = \sum_i C_i |i\rangle \,, \tag{4}$$

where $|i\rangle$ is a CMPC and C_i is the expanding coefficient.

The angular momentum alignment for the state $|\Psi\rangle$ can be written as

$$\langle\Psi|J_x|\Psi\rangle = \sum_i C_i^2 \langle i|J_x|i\rangle + 2\sum_{i<j} C_i C_j \langle i|J_x|j\rangle \,, \tag{5}$$

and the kinematic MOI is

$$J^{(1)} = \frac{1}{\omega}\langle\Psi|J_x|\Psi\rangle \,. \tag{6}$$

The experimental MOI and rotational frequency for one rotational band can be extracted by

$$\frac{J^{(1)}(I)}{\hbar^2} = \frac{2I+1}{E_\gamma(I+1\to I-1)} \,,$$
$$\hbar\omega(I) = \frac{E_\gamma(I+1\to I-1)}{I_x(I+1) - I_x(I-1)} \,, \tag{7}$$

TABLE I. Deformation parameters (ε_2, ε_4) for Pm isotopes adopted in the present PNC-CSM calculation, which are taken from Ref. [41].

	^{153}Pm	^{154}Pm	^{155}Pm	^{156}Pm	^{157}Pm
ε_2	0.250	0.250	0.258	0.258	0.267
ε_4	−0.073	−0.067	−0.060	−0.060	−0.047

separately for each signature sequence ($\alpha = I \bmod 2$), where $I_x(I) = \sqrt{(I+1/2)^2 - K^2}$, and K is the projection of the total angular momentum onto the symmetry z axis.

III. RESULTS AND DISCUSSION

In the present calculation for Pm isotopes, the parameters in the PNC-CSM are taken the same as our previous investigation for the neighboring Nd and Sm isotopes [26]. Here we show them again briefly for convenience. The deformation parameters (ε_2, ε_4) are taken from Ref. [41] (cf., Table I) and the Nilsson parameters (κ and μ) are taken as the traditional values [39]. In addition, the neutron orbital $\nu 5/2^+[642]$ is shifted upward by $0.07\hbar\omega_0$ for all Pm isotopes to reproduce the experimental single-particle level sequence. The CMPC space is constructed in proton $N = 4, 5$ major shells and neutron $N = 5, 6$ major shells, respectively. The CMPC truncation energies are about $0.85\hbar\omega_0$ for both protons and neutrons. The dimensions of the CMPC space are 1000 for both protons and neutrons. For all Pm isotopes, the monopole and quadrupole pairing strengths are chosen as $G_{0\rm p} = 0.25$ MeV and $G_{2\rm p} = 0.01$ MeV fm^{-4} for protons, and $G_{0\rm n} = 0.30$ MeV and $G_{2\rm n} = 0.02$ MeV fm^{-4} for neutrons. Note that the paring strengths in Ref. [26] are determined by the odd-even differences in nuclear binding energies of Nd and Sm isotopes (see Fig. 1 in Ref. [26]). Since these Pm isotopes are the neighbors of the Nd and Sm nuclei in Ref. [26], their pairing strengths should be similar.

The proton and neutron cranked Nilsson levels near the Fermi surface of ^{155}Pm are shown in Fig. 1. The

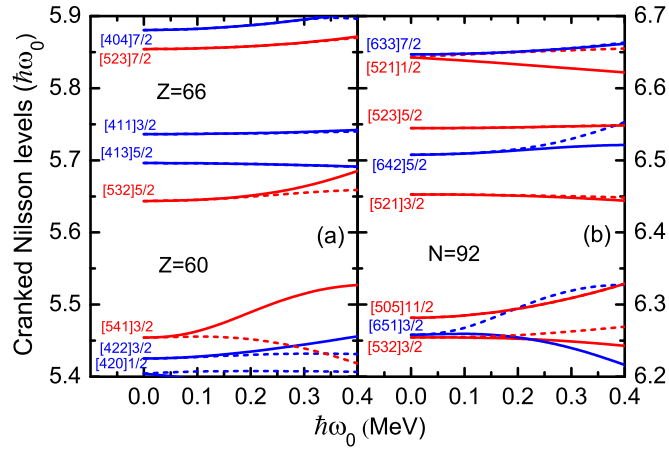

FIG. 1. The cranked single-particle levels near the Fermi surface of ^{155}Pm for (a) protons and (b) neutrons. The positive-parity (negative-parity) levels are denoted by blue (red) lines. The signature $\alpha = +1/2$ ($\alpha = -1/2$) levels are denoted by solid (dashed) lines.

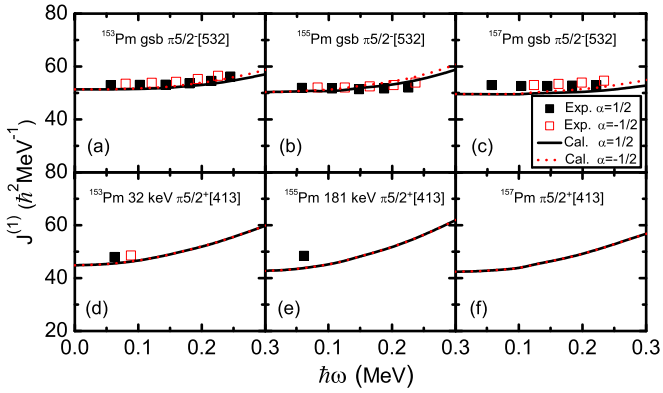

FIG. 2. The experimental [13,43,44] and calculated kinematic MOIs for the ground-state band $\pi 5/2^-[532]$ (upper panel) and the excited-state band $\pi 5/2^+[413]$ (lower panel) in ^{153,155,157}Pm.

single-particle level structures for all Pm isotopes considered in the present work are very close to each other, so we only show ^{155}Pm as an example. The present calculation shows that the ground states for ^{153,155,157}Pm are all $\pi 5/2^-[532]$, which is consistent with the experimental data [13,18,20]. In addition, for the neighboring nuclei Nd and Sm, the experimental data show that the ground states for $N = 93$ isotones (^{153}Nd and ^{155}Sm) are $\nu 3/2^-[521]$ [42,43], which is also reproduced by the present calculation. Therefore, the cranked Nilsson levels adopted here are quite reasonable.

Figure 2 shows the comparison between experimental [13,43,44] and calculated kinematic MOIs for the ground-state band (GSB) $\pi 5/2^-[532]$ (upper panel) and the excited-state band $\pi 5/2^+[413]$ (lower panel) in ^{153,155,157}Pm. It can be seen in Fig. 2 that all the experimental MOIs can be reproduced quite well by PNC-CSM except $\pi 5/2^+[413]$ in ^{155}Pm, which are a little underestimated by the calculation. In addition, the signature splittings in $\pi 5/2^-[532]$ are also well reproduced. Thus, the present calculation in turn supports the configuration assignments for these 1-qp bands in Ref. [13]. Note that the parameter set we adopted in the present PNC-CSM calculation can also reproduce the rotational bands in the neighboring Nd and Sm isotopes, including both even-even and odd-A nuclei [26]. Therefore, PNC-CSM is reliable to make the configuration and bandhead spin assignments for the 2-qp bands observed in odd-odd ^{154,156}Pm [13].

Figure 3 shows the experimental level scheme of three 2-qp bands observed in ^{154}Pm and ^{156}Pm. The data are taken from Ref. [13]. For ^{154}Pm, two isomers with half-lives of 2.68- and 1.73-min were observed several years ago [45]. In Ref. [46], using the quasiparticle-rotor model, the 2.68- and 1.73-min isomers have been assigned as 2-qp with the configurations $K^\pi = 4^+$ ($\pi 5/2^-[532] \otimes \nu 3/2^-[521]$) and $K^\pi = 1^-$ ($\pi 5/2^+[413] \otimes \nu 3/2^-[521]$), respectively. In addition, the configurations for several levels have also been assigned in Ref. [46]. For ^{156}Pm, the 26.7-sec ground state and one isomeric state with 150.3 keV have been observed by a previous experiment [47]. In Refs. [21,22], they are interpreted as one Gallagher-Moszkowski (GM) doublet with $K^\pi = 4^+$ and 1^+ ($\pi 5/2^-[532] \otimes \nu 3/2^-[521]$), whereas in Ref. [48], the ground state of ^{156}Pm is assumed to have the configuration $K^\pi = 4^-$ ($\pi 5/2^+[413] \otimes \nu 3/2^-[521]$). The three 2-qp rotational bands observed in Ref. [13] may either be established above these isomeric states or above other excited states which are close to these isomeric states with energy. Because of the lack of firm spin and parity assignments, reasonable configuration assignments have not been made for these three 2-qp bands [13]. Therefore, all the lowest spins in

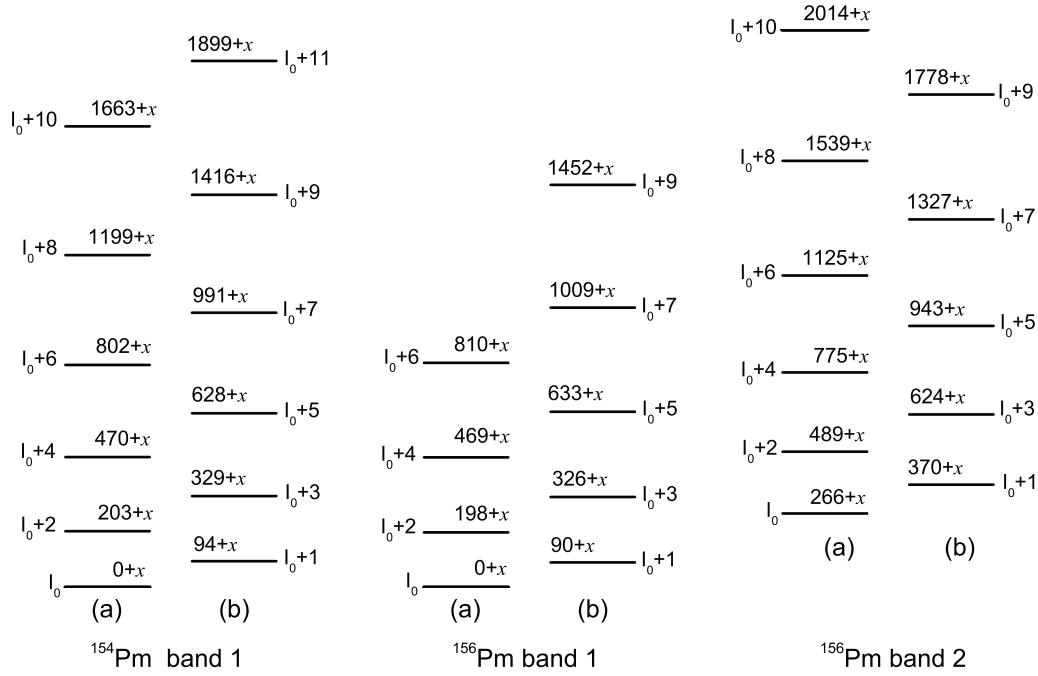

FIG. 3. The experimental level scheme of the three 2-qp bands in ^{154}Pm and ^{156}Pm. The data are taken from Ref. [13].

TABLE II. The possible low-lying 2-qp configurations in ^{154,156}Pm and the corresponding K quantum numbers. The stars are added after the GM favored K values.

	Configuration	$K_>$	$K_<$
Conf1	$\pi 5/2^-[532] \otimes \nu 3/2^-[521]$	4*	1
Conf2	$\pi 5/2^-[532] \otimes \nu 5/2^+[642]$	5*	0
Conf3	$\pi 5/2^-[532] \otimes \nu 5/2^-[523]$	5	0*
Conf4	$\pi 5/2^+[413] \otimes \nu 3/2^-[521]$	4	1*
Conf5	$\pi 5/2^+[413] \otimes \nu 5/2^+[642]$	5	0*
Conf6	$\pi 5/2^+[413] \otimes \nu 5/2^-[523]$	5*	0

these three bands are assumed as I_0 with energy $0 + x$. Note that the 2-qp band in ^{152}Pm observed in Ref. [13] does not show a typical rotational character, so we only focus on the three 2-qp bands in ^{154}Pm and ^{156}Pm. In the following, the configurations and bandhead spins will be assigned for them.

For the deformed odd-odd nucleus, when one unpaired proton and one unpaired neutron are coupled, the projections of their total angular momentum on the symmetry axis (Ω_p and Ω_n) can produce two states with $K_> = |\Omega_p + \Omega_n|$ and $K_< = |\Omega_p - \Omega_n|$ due to the residual proton-neutron interaction. They follow the GM coupling rules [49]

$$K_> = |\Omega_p + \Omega_n|, \quad \text{if } \Omega_p = \Lambda_p \pm \tfrac{1}{2} \text{ and } \Omega_n = \Lambda_n \pm \tfrac{1}{2},$$
$$K_< = |\Omega_p - \Omega_n|, \quad \text{if } \Omega_p = \Lambda_p \pm \tfrac{1}{2} \text{ and } \Omega_n = \Lambda_n \mp \tfrac{1}{2}.$$

Table II shows the possible low-lying 2-qp configurations in ^{154,156}Pm and the corresponding K quantum numbers. The stars are added after the GM favored K values. For convenience, these configurations are referred as Conf1 to Conf6, respectively.

It can be seen from Eq. (7) that for one rotational band, the extracted MOIs with rotational frequency are very sensitive to the bandhead spin. Changing the K value for one rotational band can only affect the extracted rotational frequency. Therefore, first we can assign different bandhead spins and K values to these three 2-qp bands and extract the variation of the MOIs with rotational frequency. Then by comparison with the PNC-CSM calculations using different configurations, the configurations and bandhead spins of these 2-qp bands can be obtained. Note that the bandhead spin of the GSB in the superheavy nucleus ^{256}Rf has already been assigned successfully by PNC-CSM using this method [50]. In addition, $E2$ transitions are also quite important to the configuration assignment for a rotational band. In cranking calculations, the $E2$ transitions cannot be calculated in a quantum mechanical way. However, the semiclassical approximations have been extensively used in describing various novel rotations, such as the magnetic, antimagnetic, and chiral rotations [51–56]. If the configurations of these novel rotations are assigned properly, good agreements with the data can be achieved. Since there is no experimental $E2$ transition in these Pm isotopes, in the present work, only kinematic MOIs are adopted for the configuration and bandhead spin assignments.

Figure 4 shows the comparison between the experimental and calculated kinematic MOIs for the 2-qp rotational band in ^{154}Pm (cf., the left column of Fig. 3) with different bandhead spin assignments I_0 using the configuration (a) $\pi 5/2^-[532] \otimes \nu 3/2^-[521]$, (b) $\pi 5/2^-[532] \otimes \nu 5/2^+[642]$, (c) $\pi 5/2^+[413] \otimes \nu 3/2^-[521]$, and (d) $\pi 5/2^+[413] \otimes \nu 5/2^+[642]$. Note that the proton-neutron residual interaction is not taken into account in the PNC-CSM, so it is hard to assign the K quantum numbers for these 2-qp configurations. Since this 2-qp rotational band may be established above the ground state of ^{154}Pm, the GM favored coupling mode (cf., Table II) is adopted when extracting the experimental data by Eq. (7). It can be seen clearly in Fig. 4 that the configuration $\pi 5/2^-[532] \otimes \nu 3/2^-[521]$ [Fig. 4(a)] can reproduce the extracted MOIs quite well if the bandhead spin is assigned as $I_0 = 4\hbar$. In addition, the experimental MOIs show a small signature splitting, which is also reproduced quite well by the PNC-CSM calculations [$\pi 5/2^-[532](\alpha = \pm 1/2) \otimes \nu 3/2^-[521](\alpha = -1/2)$]. For other configurations [Figs. 4(b), 4(c), and 4(d)], no matter which bandhead spin is assigned, all the calculations cannot reproduce the extracted MOIs. This demonstrates that the configuration of this 2-qp rotational band in ^{154}Pm is $\pi 5/2^-[532] \otimes \nu 3/2^-[521]$, and the corresponding bandhead spin is $I_0 = 4\hbar$. It also can be seen from the cranked Nilsson levels in Fig. 1 that this configuration corresponds to the ground state in ^{154}Pm. According to the GM coupling rules, the favored K value for this configuration is $K_> = 4$. Note that in Ref. [46], the 2.68-min isomer in ^{154}Pm is assigned as the ground state with the same configuration $K^\pi = 4^+$.

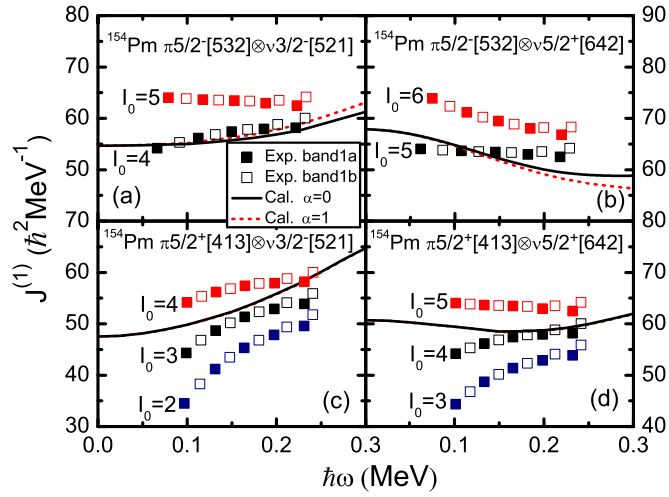

FIG. 4. The comparison between the experimental and calculated kinematic MOIs for the 2-qp band in ^{154}Pm (cf., the left column of Fig. 3) with different bandhead spin assignments I_0 using the configuration (a) $\pi 5/2^-[532] \otimes \nu 3/2^-[521]$, (b) $\pi 5/2^-[532] \otimes \nu 5/2^+[642]$, (c) $\pi 5/2^+[413] \otimes \nu 3/2^-[521]$, and (d) $\pi 5/2^+[413] \otimes \nu 5/2^+[642]$. The GM favored coupling mode (cf., Table II) is chosen for each configuration assignment. The extracted experimental MOIs far away from the PNC-CSM calculation are not shown.

Figure 5 is similar to Fig. 4, but for the band 1 in ^{156}Pm (cf., the middle column of Fig. 3). It can be seen that the configuration $\pi 5/2^-[532] \otimes \nu 3/2^-[521]$ [Fig. 5(a)] can reproduce the extracted MOIs quite well with the bandhead spin $I_0 = 4\hbar$. According to the GM coupling rules, the favored

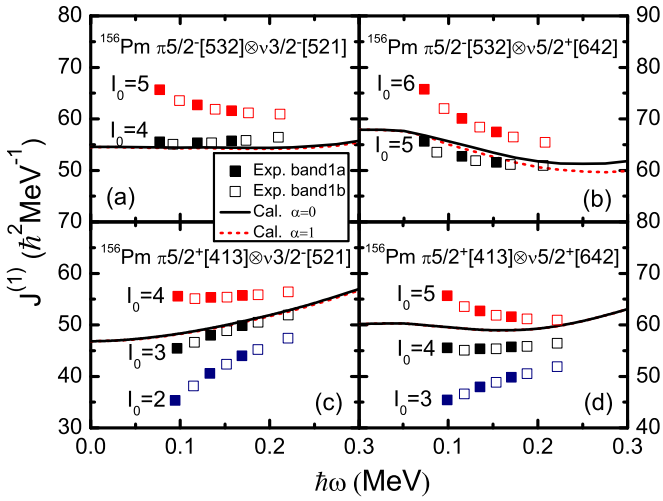

FIG. 5. Similar with Fig. 4, but for the band 1 in ^{156}Pm (cf., the middle column of Fig. 3).

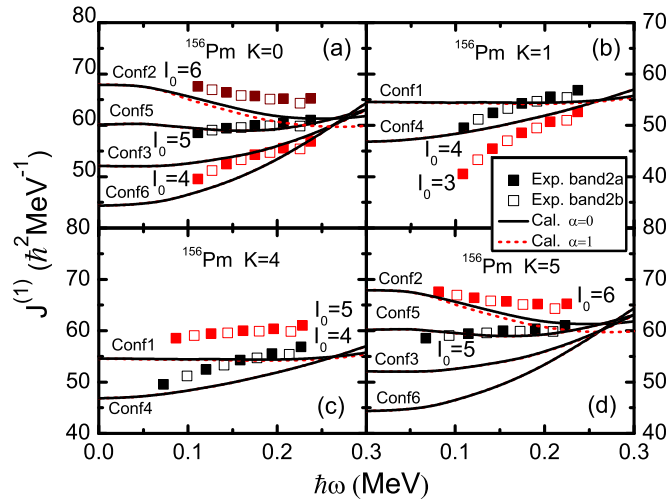

FIG. 6. The comparison between the experimental and calculated kinematic MOIs for the band 2 in ^{156}Pm (cf., the right column of Fig. 3) with different bandhead spin assignments using the configurations with (a) $K = 0$, (b) $K = 1$, (c) $K = 4$, and (d) $K = 5$. The denotations for these configurations can be seen in Table II.

K value for this configuration is $K_> = 4$. We can get that it has the same configuration as the 2-qp band in ^{154}Pm. In addition, this band shows nearly no signature splitting, which is different from the 2-qp band in ^{154}Pm. This indicates that band 1 in ^{156}Pm is coupled from the favored signature of the odd proton ($\alpha = -1/2$) with $\alpha = \pm 1/2$ of the odd neutron to form the total signature $\alpha = 0, 1$. Note that although the configuration $\pi 5/2^-[532] \otimes \nu 5/2^+[642]$ seems to approximately reproduce the extracted MOIs with bandhead spin $I_0 = 5\hbar$, an obvious signature splitting exists in the calculated MOIs, which is inconsistent with the data. This is because both $\pi 5/2^-[532]$ and $\nu 5/2^+[642]$ have signature splittings; no matter how they are coupled, an obvious signature splitting always exists. It also can be seen from the cranked Nilsson levels in Fig. 1 that this configuration corresponds to the ground state in ^{156}Pm. The experimental data show that the ground states of $N = 93$ isotones (^{153}Nd and ^{155}Sm) are $\nu 3/2^-[521]$. From a systematic point of view, with two neutrons increasing, the ground state of $N = 95$ isotones should be $\nu 5/2^+[642]$. However, in Ref. [57] the data show that the ground state of ^{155}Nd is $\nu 3/2^-[521]$. Therefore, whether this state is the ground state or not still needs further investigation. Note that in Refs. [21,22], the 26.7-sec ground state is interpreted as $K^\pi = 4^+$ ($\pi 5/2^-[532] \otimes \nu 3/2^-[521]$).

Since the band 2 in ^{156}Pm (cf., the right column of Fig. 3) is not established above the ground state, in Fig. 6, we have calculated all possible low-lying 2-qp configurations with different bandhead spin assignments and compared with the extracted MOIs by assigning (a) $K = 0$, (b) $K = 1$, (c) $K = 4$, and (d) $K = 5$. The denotations for these configurations can be seen in Table II. It can be seen that the configuration $\pi 5/2^+[413] \otimes \nu 5/2^+[642]$ [Figs. 6(a) and 6(d)] can reproduce the extracted MOIs very well with the bandhead spin $I_0 = 5\hbar$, no matter the K quantum number is assigned as 5 or 0. According to the GM coupling rules, the favored K value is 0 for this configuration. However, if $K = 0$ is assigned, the bandhead should be $I = 0$, which is too far away from the assigned bandhead $I = 5\hbar$. Therefore, we tentatively assign this configuration with $K = 5$. It also can be seen that the experimental data show quite small signature splitting. This indicates that band 2 in ^{156}Pm is coupled from the favored signature of the odd neutron ($\alpha = 1/2$) with $\alpha = \pm 1/2$ of the odd proton to form the total signature $\alpha = 0, 1$.

Finally, we have made proper configuration and bandhead spin assignments for these three 2-qp rotational bands in ^{154,156}Pm by PNC-CSM. In addition, it can be seen in Figs. 4, 5, and 6 that the calculated MOIs for the 2-qp rotational bands are quite different with different configurations. Therefore, they may provide the information on the configuration and bandhead spin to the rotational bands observed in further experiments.

IV. SUMMARY

In summary, the recently observed rotational bands in the neutron-rich nuclei $^{153–157}$Pm are investigated by a particle-number-conserving method. The kinematic moments of inertia for the one-quasiparticle bands in ^{153,155,157}Pm are reproduced very well by the calculation. Configuration and bandhead spin assignments have been made for the three two-quasiparticle bands in ^{154,156}Pm by comparison of the experimental and calculated moments of inertia. For the two-quasiparticle band in ^{154}Pm, the configuration is assigned as $\pi 5/2^-[532] \otimes \nu 3/2^-[521]$ ($K^\pi = 4^+$) with the bandhead spin $I_0 = 4\hbar$. In ^{156}Pm, the configurations of the two two-quasiparticle bands are assigned as $\pi 5/2^-[532] \otimes \nu 3/2^-[521]$ ($K^\pi = 4^+$) with the bandhead spin $I_0 = 4\hbar$, and $\pi 5/2^+[413] \otimes \nu 5/2^+[642]$ ($K^\pi = 5^+$) with the bandhead spin $I_0 = 5\hbar$, respectively. Meanwhile, the moments of inertia for several possible low-lying two-quasiparticle bands in ^{154,156}Pm have also been calculated, which are quite different from each other. Therefore, these calculated results also provide valuable information on the configuration and bandhead spin to further experiments about these two odd-odd nuclei.

ACKNOWLEDGMENTS

This work is supported by National Natural Science Foundation of China (Grants No. 11875027, No. 11775112, No. 11775026, No. 11775099, and No. 11975096), Fundamental Research Funds for the Central Universities (Grant No. 2018MS058), and the program of China Scholarships Council (Grant No. 201850735020).

[1] J. H. Hamilton, A. V. Ramayya, S. J. Zhu, G. M. Ter-Akopian, Y. T. Oganessian, J. D. Cole, J. O. Rasmussen, and M. A. Stoyer, Prog. Part. Nucl. Phys. **35**, 635 (1995).

[2] J. H. Hamilton, A. V. Ramayya, J. K. Hwang, J. Kormicki, B. R. S. Babu, A. Sandulescu, A. Florescu, W. Greiner, G. M. Ter-Akopian, Y. T. Oganessian *et al.*, Prog. Part. Nucl. Phys. **38**, 273 (1997).

[3] G. Andersson, S. E. Larsson, G. Leander, P. Möller, S. G. Nilsson, I. Ragnarsson, S. Åberg, R. Bengtsson, J. Dudek, B. Nerlo-Pomorska *et al.*, Nucl. Phys. A **268**, 205 (1976).

[4] R. Bengtsson and S. Frauendorf, Nucl. Phys. A **327**, 139 (1979).

[5] W. Nazarewicz, J. Dudek, R. Bengtsson, T. Bengtsson, and I. Ragnarsson, Nucl. Phys. A **435**, 397 (1985).

[6] J. Dobaczewski and J. Dudek, Comput. Phys. Commun. **102**, 166 (1997).

[7] A. V. Afanasjev, J. König, and P. Ring, Nucl. Phys. A **608**, 107 (1996).

[8] H. Hara and Y. Sun, Int. J. Mod. Phys. E **4**, 637 (1995).

[9] W. Urban, J. Durell, W. Phillips, B. Varley, C. Hess, M. Jones, C. Pearson, W. Vermeer, C. Vieu, J. Dionisio, M. Pautrat, and J. Bacelar, Nucl. Phys. A **587**, 541 (1995).

[10] M. Jones, W. Urban, J. Durell, M. Leddy, W. Phillips, B. Varley, P. Dagnall, A. Smith, D. Thompson, C. Vieu *et al.*, Nucl. Phys. A **609**, 201 (1996).

[11] W. J. Vermeer, M. K. Khan, A. S. Mowbray, J. B. Fitzgerald, J. A. Cizewski, B. J. Varley, J. L. Durell, and W. R. Phillips, Phys. Rev. C **42**, R1183 (1990).

[12] W. Urban, J. Bacelar, W. Gast, G. Hebbinghaus, A. Krämer-Flecken, R. Lieder, T. Morek, and T. Rzaąca-Urban, Phys. Lett. B **247**, 238 (1990).

[13] S. Bhattacharyya, E. H. Wang, A. Navin, M. Rejmund, J. H. Hamilton, A. V. Ramayya, J. K. Hwang, A. Lemasson, A. V. Afanasjev, S. Bhattacharya *et al.*, Phys. Rev. C **98**, 044316 (2018).

[14] W. R. Daniels and D. C. Hoffman, Phys. Rev. C **4**, 919 (1971).

[15] J. D'auria, D. Ostrom, and S. Gujrathi, Nucl. Phys. A **178**, 172 (1971).

[16] T. Karlewski, N. Hildebrand, G. Herrmann, N. Kaffrell, N. Trautmann, and M. Brügger, Z. Phys. A **322**, 177 (1985).

[17] R. C. Greenwood, R. A. Anderl, J. D. Cole, and H. Willmes, Phys. Rev. C **35**, 1965 (1987).

[18] A. Taniguchi, T. Ikuta, A. Osa, H. Yamamoto, K. Kawade, J.-Z. Ruan, S. Yamada, Y. Kawase, and K. Okano, J. Phys. Soc. Jpn. **65**, 3824 (1996).

[19] M. Shibata, O. Suematsu, Y. Kojima, K. Kawade, A. Taniguchi, and Y. Kawase, Eur. Phys. J. A **31**, 171 (2007).

[20] J. K. Hwang, A. V. Ramayya, J. H. Hamilton, S. H. Liu, K. Li, H. L. Crowell, C. Goodin, Y. X. Luo, J. O. Rasmussen, and S. J. Zhu, Phys. Rev. C **80**, 037304 (2009).

[21] P. C. Sood, M. Sainath, R. Gowrishankar, and K. V. Sai, Phys. Rev. C **83**, 027303 (2011).

[22] P. C. Sood, K. V. Sai, R. Gowrishankar, and M. Sainath, Phys. Rev. C **83**, 057302 (2011).

[23] P. Sood, M. Sainath, R. Gowrishankar, and B. Singh, Eur. Phys. J. A **48**, 136 (2012).

[24] J. Y. Zeng and T. S. Cheng, Nucl. Phys. A **405**, 1 (1983).

[25] J. Y. Zeng, T. H. Jin, and Z. J. Zhao, Phys. Rev. C **50**, 1388 (1994).

[26] Z.-H. Zhang, Phys. Rev. C **98**, 034304 (2018).

[27] X.-T. He and Y.-C. Li, Phys. Rev. C **98**, 064314 (2018).

[28] C. S. Wu and J. Y. Zeng, Phys. Rev. C **39**, 666 (1989).

[29] X. M. Fu, F. R. Xu, J. C. Pei, C. F. Jiao, Y. Shi, Z. H. Zhang, and Y. A. Lei, Phys. Rev. C **87**, 044319 (2013).

[30] J. Meng, J.-Y. Guo, L. Liu, and S.-Q. Zhang, Front. Phys. China **1**, 38 (2006).

[31] Z. Shi, Z. H. Zhang, Q. B. Chen, S. Q. Zhang, and J. Meng, Phys. Rev. C **97**, 034317 (2018).

[32] W. Y. Liang, C. F. Jiao, Q. Wu, X. M. Fu, and F. R. Xu, Phys. Rev. C **92**, 064325 (2015).

[33] R. Richardson and N. Sherman, Nucl. Phys. **52**, 221 (1964).

[34] F. Pan, J. Draayer, and W. Ormand, Phys. Lett. B **422**, 1 (1998).

[35] A. Volya, B. A. Brown, and V. Zelevinsky, Phys. Lett. B **509**, 37 (2001).

[36] L. Y. Jia, Phys. Rev. C **88**, 044303 (2013).

[37] L. Y. Jia, Phys. Rev. C **88**, 064321 (2013).

[38] W.-C. Chen, J. Piekarewicz, and A. Volya, Phys. Rev. C **89**, 014321 (2014).

[39] S. G. Nilsson, C. F. Tsang, A. Sobiczewski, Z. Szymański, S. Wycech, C. Gustafson, I. L. Lamm, P. Möller, and B. Nilsson, Nucl. Phys. A **131**, 1 (1969).

[40] H. Molique and J. Dudek, Phys. Rev. C **56**, 1795 (1997).

[41] P. Möller and J. Nix, At. Data Nucl. Data Tables **59**, 185 (1995).

[42] J. K. Hwang, A. V. Ramayya, J. H. Hamilton, J. Kormicki, L. K. Peker, B. R. S. Babu, T. N. Ginter, G. M. Ter-Akopian, Y. T. Oganessian, A. V. Daniel *et al.*, Int. J. Mod. Phys. E **06**, 331 (1997).

[43] C. W. Reich, Nucl. Data Sheets **104**, 1 (2005).

[44] R. Helmer, Nucl. Data Sheets **107**, 507 (2006).

[45] C. W. Reich, Nucl. Data Sheets **110**, 2257 (2009).

[46] P. C. Sood, R. Gowrishankar, and K. V. Sai, J. Phys. G: Nucl. Part. Phys. **39**, 095107 (2012).

[47] C. W. Reich, Nucl. Data Sheets **99**, 753 (2003).

[48] M. Hellström, B. Fogelberg, L. Spanier, and H. Mach, Phys. Rev. C **41**, 2325 (1990).

[49] C. J. Gallagher and S. A. Moszkowski, Phys. Rev. **111**, 1282 (1958).

[50] Z.-H. Zhang, J. Meng, E.-G. Zhao, and S.-G. Zhou, Phys. Rev. C **87**, 054308 (2013).

[51] P. W. Zhao, S. Q. Zhang, J. Peng, H. Z. Liang, P. Ring, and J. Meng, Phys. Lett. B **699**, 181 (2011).

[52] P. W. Zhao, J. Peng, H. Z. Liang, P. Ring, and J. Meng, Phys. Rev. Lett. **107**, 122501 (2011).
[53] P. W. Zhao, J. Peng, H. Z. Liang, P. Ring, and J. Meng, Phys. Rev. C **85**, 054310 (2012).
[54] J. Meng, J. Peng, S.-Q. Zhang, and P.-W. Zhao, Front. Phys. **8**, 55 (2013).
[55] P. W. Zhao, S. Q. Zhang, and J. Meng, Phys. Rev. C **92**, 034319 (2015).
[56] P. Zhao, Phys. Lett. B **773**, 1 (2017).
[57] J. K. Hwang, A. V. Ramayya, J. H. Hamilton, K. Li, C. Goodin, Y. X. Luo, J. O. Rasmussen, and S. J. Zhu, Phys. Rev. C **78**, 014309 (2008).